# FINAL SCIENTIFIC/TECHNICAL REPORT

DOE Award: #DE-SC0005362

Western Michigan University

Project Title: Development of Surface Complexation Models of Cr(VI) Adsorption on Soils, Sediments and Model Mixtures of Kaolinite, Montmorillonite, γ-Alumina, Hydrous Manganese and Ferric Oxides and Goethite

PI: Dr. Carla M. Koretsky

## EXECUTIVE SUMMARY

Hexavalent chromium is a highly toxic contaminant that has been introduced into aquifers and shallow sediments and soils via many anthropogenic activities. Hexavalent chromium contamination is a problem or potential problem in the shallow subsurface at several DOE sites, including Hanford, Idaho National Laboratory, Los Alamos National Laboratory and the Oak Ridge Reservation (DOE, 2008). To accurately quantify the fate and transport of hexavalent chromium at DOE and other contaminated sites, robust geochemical models, capable of correctly predicting changes in chromium chemical form resulting from chemical reactions occurring in subsurface environments are needed. One important chemical reaction that may greatly impact the bioavailability and mobility of hexavalent chromium in the subsurface is chemical binding to the surfaces of particulates, termed adsorption or surface complexation. Quantitative thermodynamic surface complexation models have been derived that can correctly calculate hexavalent chromium adsorption on well-characterized materials over ranges in subsurface conditions, such pH and salinity. However, models have not yet been developed for hexavalent chromium adsorption on many important constituents of natural soils and sediments, such as clay minerals. Furthermore, most of the existing thermodynamic models have been developed for relatively simple, single solid systems and have rarely been tested for the complex mixtures of solids present in real sediments and soils.

In this study, the adsorption of hexavalent chromium was measured as a function of pH (3-10), salinity (0.001 to 0.1 M $NaNO_3$), and partial pressure of carbon dioxide(0-5%) on a suite of naturally-occurring solids including goethite (FeOOH), hydrous manganese oxide (MnOOH), hydrous ferric oxide ($Fe(OH)_3$), γ-alumina ($Al_2O_3$), kaolinite ($Al_2Si_2O_5(OH)_4$), and montmorillonite ($Na_3(Al, Mg)_2Si_4O_{10}(OH)_2 \cdot nH_2O$). The results show that all of these materials can bind substantial quantities of hexavalent chromium, especially at low pH. Unexpectedly, experiments with the clay minerals kaolinite and montmorillonite suggest that hexavalent chromium may interact with these solids over much longer periods of time than expected. Furthermore, hexavalent chromium may irreversibly bind to these solids, perhaps because of oxidation-reduction reactions occurring on the surfaces of the clay minerals. More work should be done to investigate and quantify these chemical reactions. Experiments conducted with mixtures of goethite, hydrous manganese oxide, hydrous ferric oxide, γ-alumina, montmorillonite and kaolinite demonstrate that it is possible to correctly predict hexavalent chromium binding in the presence of multiple minerals using thermodynamic models derived for the simpler systems. Further, these models suggest that of the six solid considered in this study, goethite is typically the solid to which most of the hexavalent chromium will bind. Experiments completed with organic-rich and organic-poor natural sediments demonstrate that in organic-rich substrates, organic matter is likely to control uptake of the hexavalent chromium. The models derived and tested in this study for hexavalent chromium binding to γ-alumina, hydrous manganese oxide, goethite, hydrous ferric oxide and clay minerals can be used to better predict changes in hexavalent chromium bioavailability and mobility in contaminated sediments and soils.

## COMPARISON OF ACTUAL ACCOMPLISHMENTS WITH STATED GOALS AND OBJECTIVES

**Research Objective 1.1: Measure Cr(VI) sorption on kaolinite, HMO, γ-alumina and montmorillonite as a function of pH, ionic strength, sorbate/sorbent ratio and $pCO_2$.**

*γ-alumina:* Cr(VI) sorption was measured as a function of pH, ionic strength, sorbate/sorbent ratio and $pCO_2$ (Reich & Koretsky, 2011).

*HMO:* Cr(VI) sorption was measured as a function of pH, ionic strength, sorbate/sorbent ratio and $pCO_2$ (MacLeod and Koretsky, 2011; MacLeod, 2013).

*Montmorillonite and Kaolinite:* Cr(VI) sorption was measured as a function of pH, ionic strength and over a limited range of sorbate/sorbent conditions. Measurements were completed to investigate kinetics and reversibility and the influence of various clay pretreatments. Data were not collected as a function of $pCO_2$ (Wyman et al., 2012; Koretsky, 2012; Koretsky et al., 2013).

**Research Objective 1.2 Develop double and triple layer surface complexation models to describe Cr(VI) adsorption on kaolinite, γ-alumina, HMO and montmorillonite.**

*γ-alumina:* Constant capacitance, double layer and triple layer models were developed to describe Cr(VI) adsorption on γ-alumina (Reich & Koretsky, 2011).

*HMO:* A double layer surface complexation model was developed to describe Cr(VI) sorption on HMO (MacLeod, 2013).

*Montmorillonite and Kaolinite:* A double layer model was developed to describe Cr(VI) sorption on montmorillonite and kaolinite over very limited conditions (Gilchrist, 2013). However, due to the lack of reversibility and strong dependence on sample pre-treatment observed in the measured edges, more comprehensive double and triple layer models have not been developed.

**Research Objective 2.1 Measure Cr(VI) sorption on mineral assemblages (HMO, kaolinite, montmorillonite, γ-alumina, HFO and goethite).**

Cr(VI) sorption has been measured on combinations of: goethite/HMO, goethite/kaolinite, goethite/montmorillonite, gothite/γ-alumina, goethite/HFO and combinations of all six solids as function of solid ratios, ionic strength and $pCO_2$ Gilchrist & Koretsky, 2012; Gilchrist, 2013).

**Research Objective 2.2 Compare measured edges on mineral assemblages to predictions using simple component additivity approach to assess mineral-mineral interactions.**

Cr(VI) sorption edges on mineral edges have been compared to predictions from a simple component additivity approach using a set of double layer surface complexation models (Gilchrist and Koretsky, 2012; Gilchrist, 2013).

**Research Objective 3.1 Measure Cr(VI) adsorption edges and isotherms on four natural sediment samples (low organic C/high FMO; high organic C/high FMO; low organic C/low FMO; high organic C/low FMO)**

Sediment was collected from Kleinstuck Marsh (high organic carbon) in Michigan and the Rifle Site (low organic carbon) in Colorado. Adsorption edges were measured on two high organic C samples from the Kleinstuck Marsh and from one low organic carbon sample from the Rifle Integrated Field Challenge Research site (Wyman et al., 2012).

**Research Objective 3.2 Measure adsorption edges and isotherms on each of the natural samples after each of four stepwise sequential extractions**

Cr(VI) adsorption edges were measured on one set of samples from the Kleinstuck Marsh (high organic matter) and on one set of samples from the Rifle Site (low organic matter) after four step-wise sequential extractions (Wyman et al., 2012).

**Research Objective 3.3. Compare partitioning of Cr(VI) onto bulk and sequentially extracted fractions of natural samples to predictions from component additivity.**

This objective is still in progress.

## HYPOTHESES

Three hypotheses were posed in this study:

**Hypothesis 1:** Double or triple layer surface complexation models can be used to accurately describe Cr(VI) adsorption on kaolinite, hydrous manganese oxide (HMO), γ-alumina and montmorillonite as a function of pH, ionic strength, $pCO_2$ and sorbate/sorbent ratio. However, the DLM approach will require ionic strength dependent stability constants to achieve the same goodness-of-fit as the TLM.

**Hypothesis 2:** Double and triple layer surface complexation models developed to describe Cr(VI) adsorption on pure solids (HMO, kaolinite, γ-alumina, montmorillonite, HFO and goethite) can be used to accurately predict Cr(VI) adsorption on mixed mineral assemblages.

**Hypothesis 3:** Cr(VI) adsorption on organic-poor sediments can be accurately predicted using a component additivity approach with hydrous manganese and ferric oxide (FMO), goethite, γ-alumina, kaolinite and montmorillonite to represent idealized endmember sorbents. However, Cr(VI) adsorption on organic-rich sediments will not be accurately predicted using this approach.

## APPROACHES AND RESULTS

*Cr(VI) adsorption on γ-alumina*

Adsorption of Cr(VI) on γ-alumina was investigated as a function of ionic strength (0.001, 0.01 and 0.1 M $NaNO_3$), pH (4-10), Cr(VI) concentration ($10^{-4}$ or $10^{-5}$ M with 5 g/l solid) and $pCO_2$ (0, atmospheric, 2.5%) using batch experiments (Figures 1-3). Rate experiments were used to assess the rate of Cr(VI) uptake and sorption reversibility. Adsorption was rapid at a pH of 3, reaching a plateau value within 5-10 min that remained unchanged for at least two days. Approximately 80-90% of the Cr(VI) desorbed within 15 min of titrating to pH 10, with 100% desorption occurring within 24 hr. Edge experiments demonstrated that Cr(VI) sorption is significant at low pH and decreases with increasing pH, with 50% of the Cr(VI) adsorbed between pH ~6.5 and 8 (Figures 1-3). Adsorption varied little with ionic strength or $pCO_2$ under most of the studied conditions. However, at low pH under high ionic strength and especially at high ionic strength and high $pCO_2$, Cr(VI) sorption on γ-alumina was suppressed. The surface area of the γ-alumina was characterized using 11-pt $N_2$ BET, with an average value of 233 $m^2/g$.

The adsorption edge data were used to parameterize constant capacitance (CCM), diffuse double layer (DLM) and triple layer (TLM) surface complexation models. The speciation software FITEQL4.0 (Herbelin and Westall, 1999, FITEQL- a computer program for determination of chemical equlibrium constants from experimental data. Dept of Chemistry Report 99-01, Oregon State University, Corvaliss, OR) was used to optimize stability constants for Cr(VI) adsorption using each measured adsorption edge. Aqueous complexation reactions and stability constants taken from the MINTEQ default thermodynamic database were included in all calculations and the Davies equation was used to calculate activities for the aqueous species. For the CCM, three distinct sets of

published values for site density, capacitance and stability constants for protionation and deprotonation were tested with three different chromate adsorption stochiometries (Reich and Koretsky, 2011). For the DLM, three other sets of published values for site density and protonation/deprotonation constants were tested with three distinct chromate adsorption stochiometries. For the TLM, five distinct sets of previously published site density, protonation/deprotonation, electrolyte adsorption stability constants and inner/outer layer capacitance values were tested with three chromate adsorption stochiometries or combinations of these. The Cr(VI) adsorption reaction stochiometries and previously published parameters resulting in the lowest average WSOS/DF values for each type of model are show in Table 1. None of the models entirely captured the full range of observed adsorption dependence on ionic strength and sorbate/sorbent ratio. In contrast to the initial hypothesis, the best fits to the full dataset were produced by the CCM. This is likely because the stability constants are ionic-strength dependent. The more sophisticated TLM, which requires the most fitting parameters, did not produce better fits than the simpler CCM or DLM approaches for the conditions tested in this study (Reich and Koretsky, 2011).

Table 1. Best model parameters with median stability constants and average errors for CCM, DLM and TLMs. $K^+$ and $K^-$ are protonation and deprotonation stability constants corresponding to reactions >AlOH + $H^+$ = $>AlOH_2^+$ and >AlOH = $>AlO^-$ + $H^+$, where >AlOH represents a surface hydroxyl site. $K^{Na+}$ and $K^{NO3-}$ are stability constants corresponding to reactions >AlOH + $Na^+$ = $>AlO^-$ _ $Na^+$ + $H^+$ and >AlOH + $H^+$ + $NO_3^-$ = $>AlOH_2^+$_$NO_3^-$ where _ indicates separation between inner and outer planes, and electrolyte ions are assumed to adsorb on the outer plane. The measured $N_2$-BET surface area of 233 $m^2/g$ was used in all model simulations.

| **Model Type** | **Site density (μmol/m²)** | **log $K^+$, log $K^-$** | **log $K^{Na+}$, log $K^{NO3-}$** | **$C_1$, $C_2$ (F/m²)** | **Surface Species** | **log K** | **WSOS/DF** |
|---|---|---|---|---|---|---|---|
| CCM | 2.16[a] | 6.7[a], -9.0[a] | N/A | 1.06[a] | $>AlOHCrO_4^{-2}$ [h] | 2.42[b], 2.52[c,d] | 14.6[e] |
| | | | | | $(>AlOH_2)_2CO_3$ [i] | 22.5[c] (19.2)[c,g], 23.0[d] (19.7)[d,g] | 12.4[f] |
| DLM | 1.49[a] | 7.3[a], -8.6[a] | N/A | N/A | $>AlOH_2CrO_4^-$ [j] | 10.3 | 35.3[e] |
| | | | | | $(>AlOH_2)_2CO_3$ [k] | 24.3 (20.8)[g] | 34.6[f] |
| TLM | 1.49[a] | 7.0[a], -8.8[a] | -8.3[a], 8.3 [a] | 1.2 [a], 0.2 [a] | $>AlOH_2^+$_$HCrO_4^-$ [l] | 18.5 | 41.4[e] |
| | | | | | $>AlOH_2^+$_$HCO_3^-$ [m] | 20.5 | 70.8[f] |

a. Toner and Sparks (1995), b. 0.001 M $NaNO_3$, c. 0.01 M $NaNO_3$, d. 0.1 M $NaNO_3$, e. average WSOS/DF for all 0 $pCO_2$ adsorption edges, f. average WSOS/DF for all 2.5% $pCO_2$ adsorption edges; g. K' calculated using MINTEQ activity convention (=K·site density/solid concentration); h. Reaction stochiometry: >AlOH + $CrO_4^{-2}$ = $>AlOHCrO_4^{-2}$, i. Reaction stochiometry: 2(>AlOH) + $CO_3^{-2}$ = $(>AlOH_2)_2CO_3$, j. Reaction stochiometry: >AlOH + $H^+$ + $CrO_4^{-2}$ = $>AlOH_2CrO_4^-$, k. Reaction stochiometry: 2(>AlOH) + $CO_3^{-2}$ = $(>AlOH_2)_2CO_3$, l. Reaction stochiometry: >AlOH + 2$H^+$ + $CrO_4^{-2}$ = $>AlOH_2^+$_$HCrO_4^-$, m. Reaction stochiometry: >AlOH + 2$H^+$ + $CO_3^{-2}$ = $>AlOH_2^+$_$HCO_3^-$

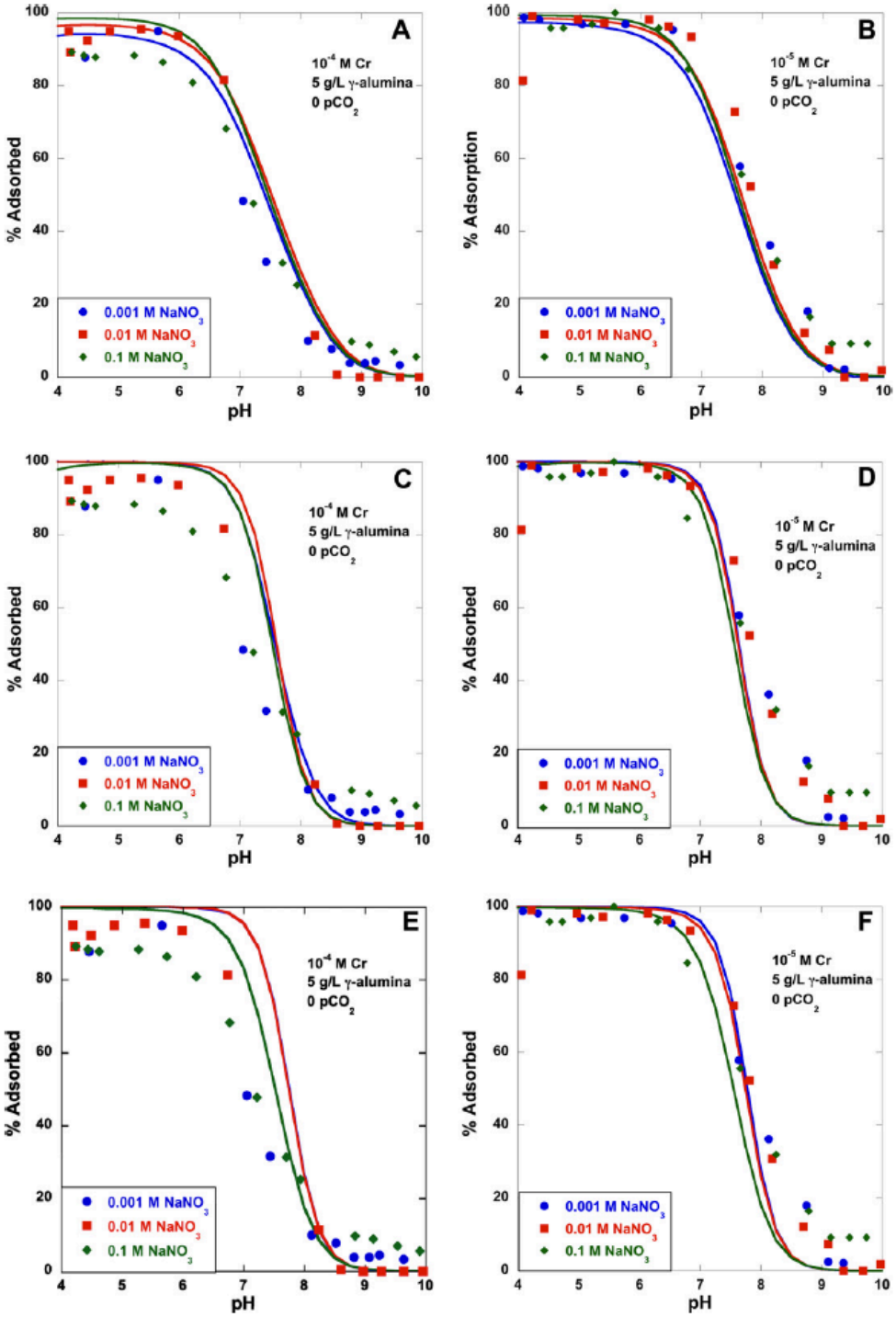


*Figure 1. Adsorption of Cr(VI) on 5 g/L of γ-alumina with 0.001 (circles), 0.01 (squares), or 0.1 (diamonds) M $NaNO_3$ in the absence of $CO_2$. Model parameters shown in Table 1 are used to calculate the adsorption edges with (A) CCM ($10^{-4}$ M Cr), (B) CCM ($10^{-5}$ M Cr), (C) DLM ($10^{-4}$M Cr), (D) DLM ($10^{-5}$ M Cr), (E) TLM ($10^{-4}$ M Cr) or (F) TLM ($10^{-5}$ M Cr).*

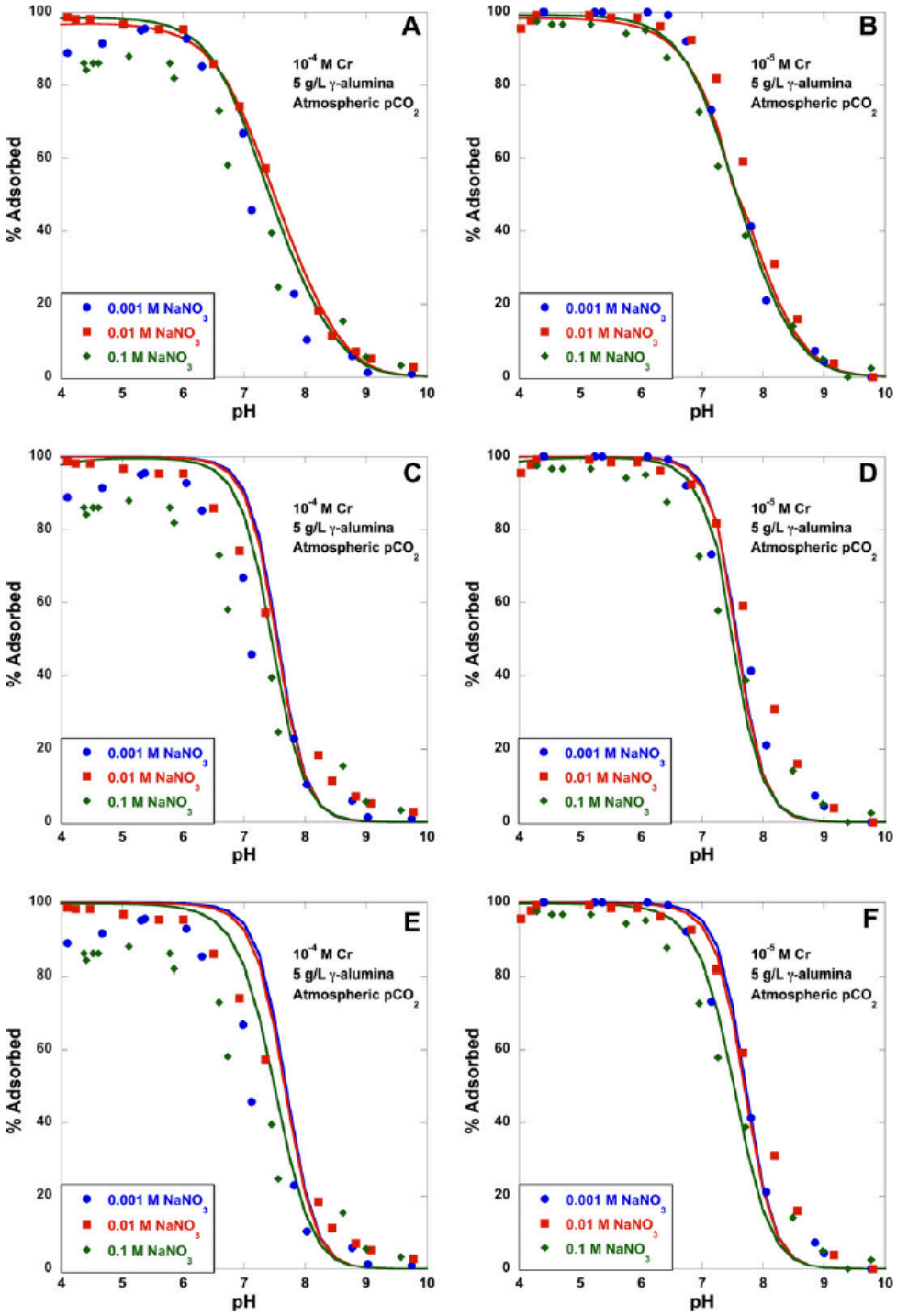


*Figure 2. Adsorption of Cr(VI) on 5 g/L of γ-alumina with 0.001 (circles), 0.01 (squares), or 0.1 (diamonds) M $NaNO_3$ in atmospheric $CO_2$. Model parameters shown in Table 1 are used to calculate the adsorption edges with (A) CCM ($10^{-4}$ M Cr), (B) CCM ($10^{-5}$ M Cr), (C) DLM ($10^{-4}$ M Cr), (D) DLM ($10^{-5}$ M Cr), (E) TLM ($10^{-4}$ M Cr) or (F) TLM ($10^{-5}$ M Cr).*

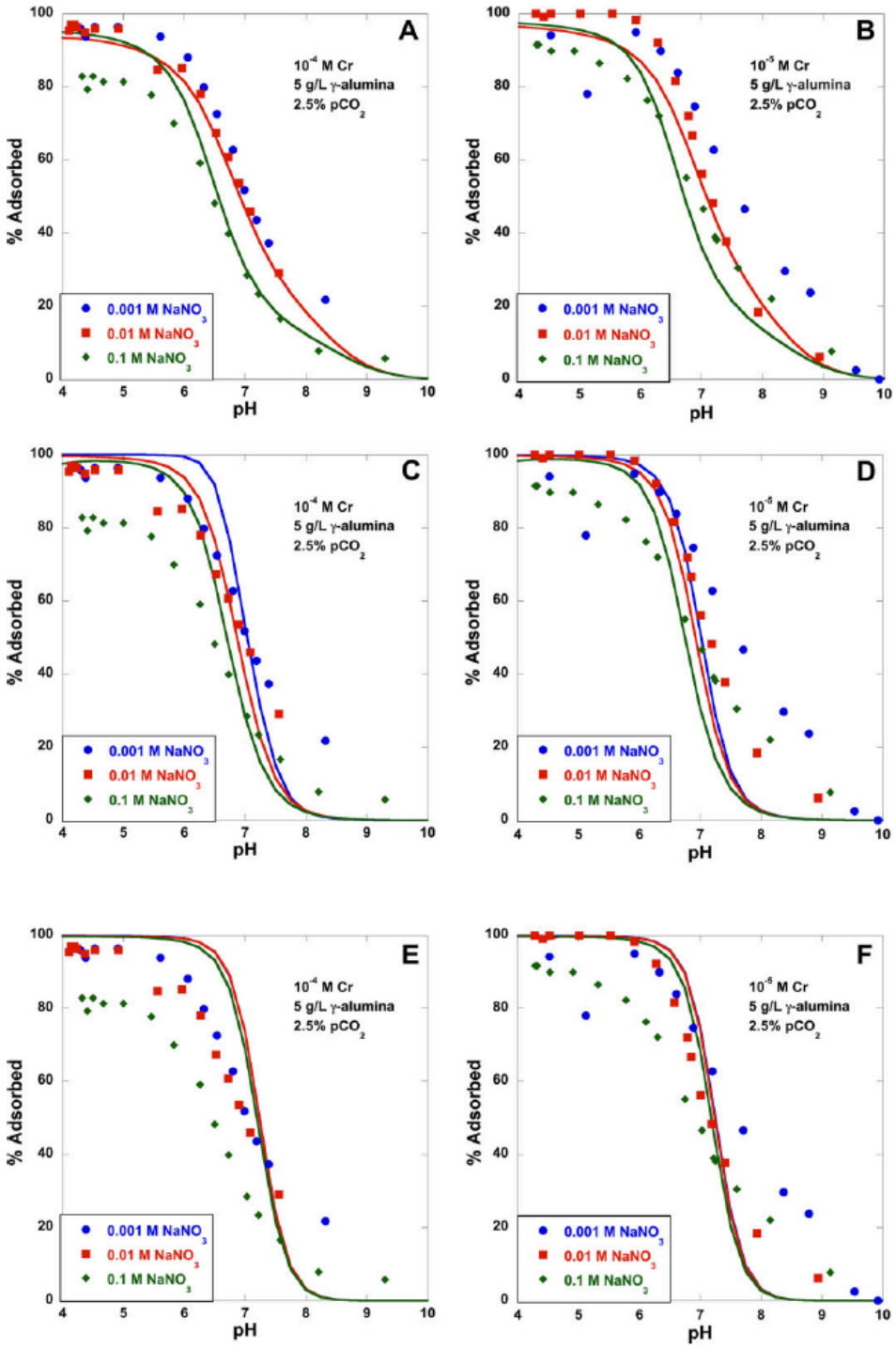


*Figure 3. Adsorption of Cr(VI) on 5 g/L of γ-alumina with 0.001 (circles), 0.01 (squares), or 0.1 (diamonds) M $NaNO_3$ in 2.5% $CO_2$. Model parameters shown in Table 1 are used to calculate the adsorption edges with (A) CCM ($10^{-4}$ M Cr), (B) CCM ($10^{-5}$ M Cr), (C) DLM ($10^{-4}$ M Cr), (D) DLM ($10^{-5}$ M Cr), (E) TLM ($10^{-4}$ M Cr) or (F) TLM ($10^{-5}$ M Cr).*

*Cr(VI) sorption on hydrous manganese oxide*

Cr(VI) adsorption edges (pH 3-10) were measured on hydrous manganese oxide (HMO) as a function of ionic strength (0.001, 0.01, and 0.1 M $NaNO_3$), $pCO_2$ (0, atmospheric, 2.5%, and 5%), Cr(VI) concentration ($10^{-5}$ or $2 \cdot 10^{-5}$ M with 5-20 g/L solid) and time (24 hrs to 2 weeks reaction time). HMO was synthesized under 0 $pCO_2$ conditions using the alkalimetric titration technique described by Stroes-Gascoyne (1987, Applied Geochemistry). The product was characterized using X-ray diffraction and the surface area analyzed using 11-pt BET (~250 $m^2/g$). Initial adsorption at pH 3 was rapid with most of the adsorption occurring within the first 10 hrs. Adsorption was readily reversible at pH 10 with >90% desorption occurring within 2 hrs of pH reversal (Figure 4A). Timed adsorption edge experiments demonstrated that most adsorption occurred at pH<6 and that Cr(VI) adsorption changed little, particularly for experiments with higher concentrations of HMO, between 4-24 hrs and 48-72 hrs equilibration time (Figure 4B). At pH < 6-7, Cr(VI) adsorption increased with decreasing pH (Figure 5) with relatively little dependence on $pCO_2$ (Figure 5A). Adsorption increased significantly, especially at low pH, with increasing ionic strength (Figure 5B).

Tonkin et al. (2004, Applied Geochemistry) developed a comprehensive two site DLM, analogous to that published by Dzombak and Morel (1990, Surface Complexation Modeling: Hydrous Ferric Oxide) for hydrous ferric oxide, to describe adsorption of a wide range of cations on hydrous manganese oxide. The site densities, site types, theoretically-derived specific surface area and deprotonation constants recommended by Tonkin et al. (2004) were used to develop a model for Cr(VI) adsorption on HMO (MacLeod, 2013). FITEQL was used to optimize stability constants for several Cr(VI) adsorption reaction stoichiometries using adsorption edges measured as a function of ionic strength under 0 $pCO_2$ conditions. Several Cr(VI) adsorption reaction stochiometries were tested; the best fit to the experimental data was produced by a model with Cr(VI) adsorption on the strong >XOH site only (Table 2; Figure 6; MacLeod, 2013). Because the relatively simple DLM provided a good fit to the experimental data, and in the case of γ-alumina (see above) performed as well as a TLM, a TLM for Cr(VI) adsorption on HMO was not developed.

Table 2. Diffuse layer model parameters used for hydrous manganese oxide.

| | |
|---|---|
| **Surface Area ($m^2/g$)** | 746[a] |
| **XOH Site Density (sites/$nm^2$)** | 1.08[a] |
| **YOH Site Density (sites/$nm^2$)** | 0.61[a] |
| **$XO^- + H^+ = XOH$** | -2.35[a] |
| **$YO^- + H^+ = YOH$** | -6.06[a] |
| **$XOH + CrO_4^{-2} = XOHCrO_4^{-2}$** | -8.57[b] |

a Tonkin et al. (2004) b. MacLeod (2013)

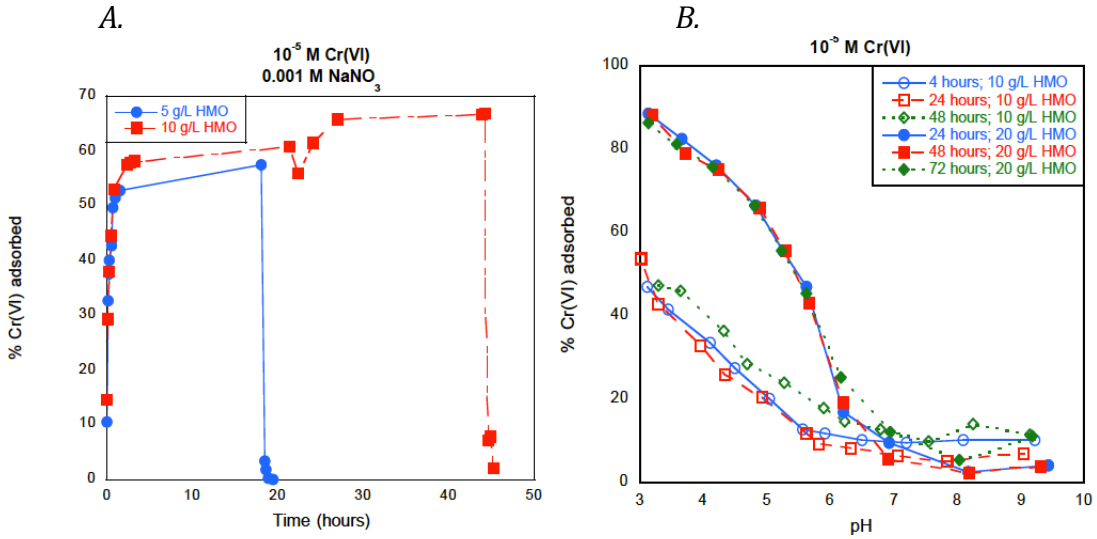


*Figure 4. (A) Cr(VI) adsorption and desorption with 5 or 10 g/L hydrous manganese oxide for systems with $10^{-5}$ M Cr(VI) in 0.001 M $NaNO_3$ as a function of time. Adsorption was completed at pH 3 and desorption at pH 10. (B) Adsorption edges for systems with $10^{-5}$ M Cr(VI) and 10 g/L HMO with 0.001 M $NaNO_3$ or 20 g/L HMO with 0.01 M $NaNO_3$ measured after 4, 24, 48 or 72 hrs equilibration time.*

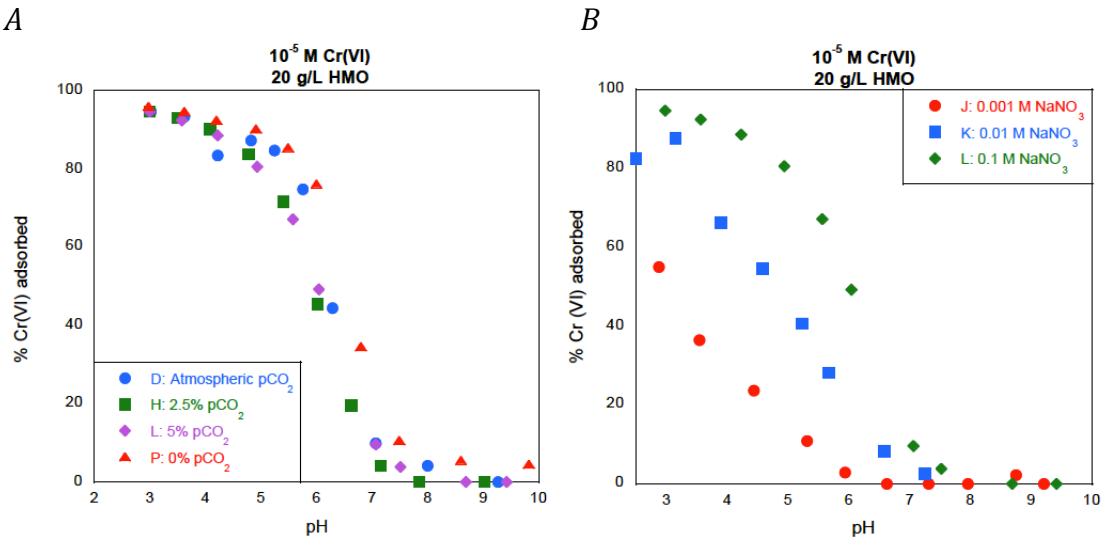


*Figure 5. Cr(VI) adsorption on 20 g/L HMO for systems with $10^{-5}$ M Cr(VI) and (A) .1 M $NaNO_3$ in 0-5% $pCO_2$ and (B) 5% $pCO_2$ with 0.001 to 0.1 M $NaNO_3$ after 24 hr equilibration time.*

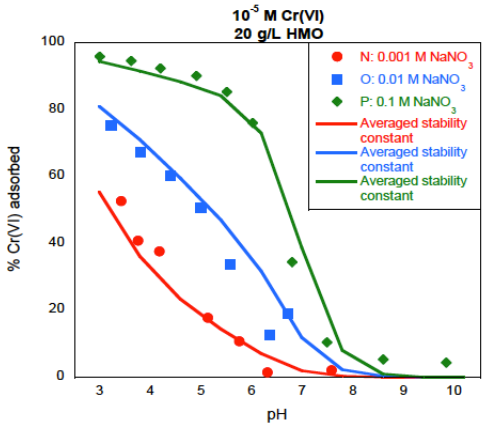


*Figure 6. Cr(VI) adsorption on 20 g/L HMO for systems with $10^{-5}$ M Cr(VI) and 0.001 to .1 M $NaNO_3$ in 0% $pCO_2$. Lines indicate DLM fits to the experimental data (MacLeod, 2013).*

*Cr(VI) sorption on kaolinite*

The kinetics of Cr(VI) adsorption on kaolinite (KGa-1b from the Clay Minerals Society) were investigated under ambient atmospheric conditions for up to 2 weeks (data not shown). For a system with 30 g/L kaolinite and $10^{-5}$ M Cr(VI) in 0.1 or 0.01 M $NaNO_3$ at a pH of 3, Cr(VI) sorption increased steadily for at least two weeks, never reaching a steady-state condition. Furthermore, sorbed Cr(VI) did not desorb from kaolinite over a period of at least 2 weeks after titrating to pH 10. Adsorption edges spanning pH 3-10 measured for a system with $10^{-5}$ M Cr(VI) on 30 g/L kaolinite in 0.01 M $NaNO_3$ in ambient atmospheric conditions also showed continuous slow uptake of Cr(VI) at acidic pH (Figure 7A). Above pH 7, Cr(VI) adsorption decreased steadily with increasing pH and changed little for reaction times varying from 24 hrs to 2 weeks. Total Cr in solution was measured using ICP-MS, and Cr(VI) in solution was measured using the diphenylcarbizide colorimetric method. No difference was observed, within experimental error, between the two datasets, demonstrating that all Cr in solution was hexavalent.

We hypothesized that reaction with Fe(II) in the crystal lattice of the kaolinite resulted in the slow, continuous sorption of Cr(VI) at low pH. To test this, Cr(VI) sorption edges were measured as a function of time (24 hrs to 2 weeks) after kaolinite was pretreated with 0.5 M HCl, 0.04 hydroxylamine HCl in 25% acetic acid or 30% $H_2O_2$ in 0.02 M $HNO_3$ (Figure 7B-D). These reagents were used to selectively dissolve or reductively dissolve Fe oxides (HCl and hydroxylamine HCl) or to oxidize and remove organic matter (peroxide). Pretreatment with HCl dramatically increased both the kinetics of Cr(VI) sorption at low pH and also the total quantity of Cr(VI) sorbed on the kaolinite, with a maximum of ~80% sorbed at pH 3 and only a slight increase in total sorption occurring between 24 hrs and 2 weeks reaction time (Figure 7B). The amount of Cr(VI) sorbed decreased nearly linearly with pH on the HCl-treated kaolinite to <5% at pH 10. In contrast, pretreatment with hydroxylamine HCl resulted in greater total sorption (100% at pH 3 after 2 weeks) with sorption increasing steadily for up to 2 weeks at pH <7. The hydroxylamine HCl may have generated additional Fe(II), which could account for the greater quantity of Cr(VI) sorbed and the continuous increase in sorbed Cr(VI) over the two week period. Surprisingly, pretreatment with peroxide also increased the rate of Cr(VI) sorption and the total quantity of Cr(VI) sorbed at pH <7 (Figure 7D). For all preteatments, dissolved Cr in solution was present as Cr(VI). Thus, any Cr(VI) reduction must result in sorbed Cr(III), rather than aqueous Cr(III). These results warrant further examination, for example by coupling the bulk measurements to XAS and Mossbauer spectroscopy data.

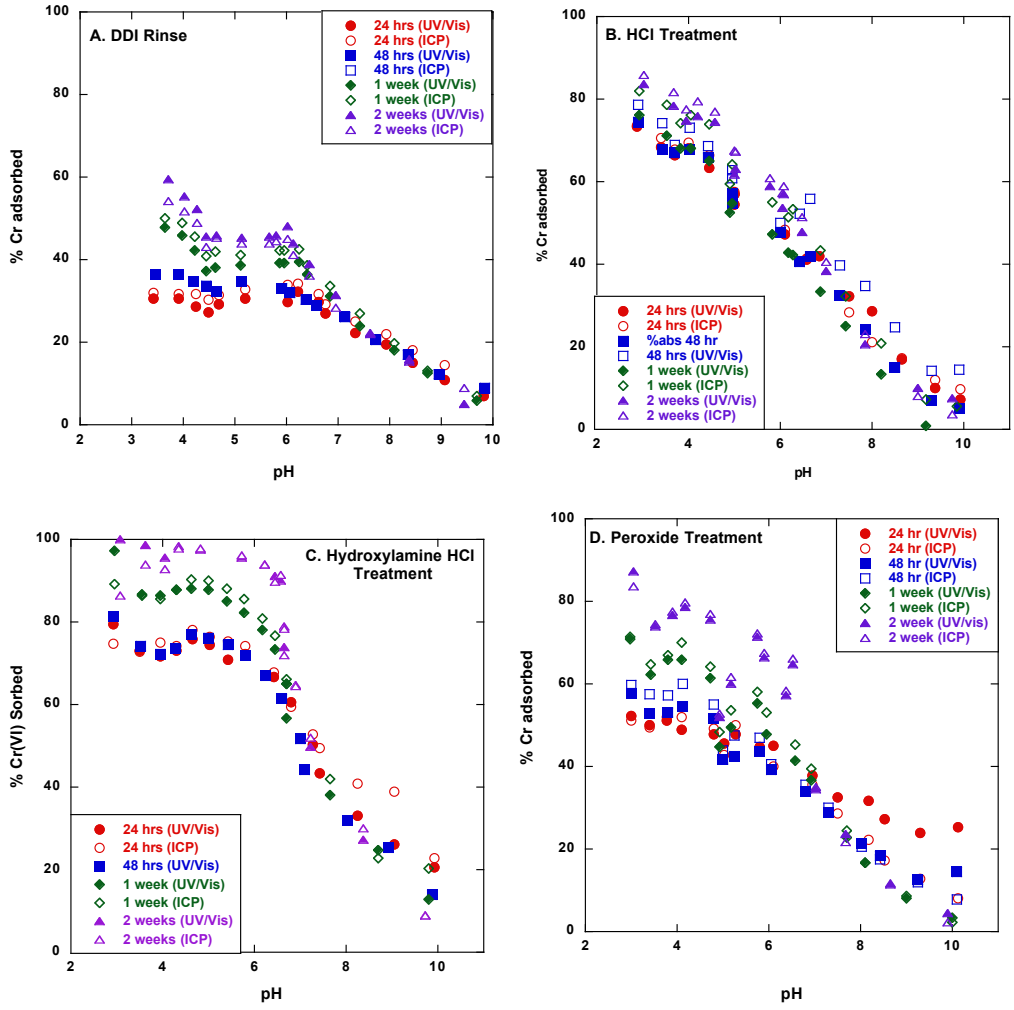


*Figure 7. Cr(VI) adsorption on 30 g/L kaolinite for systems with $10^{-5}$ M Cr(VI) and 0.01 M $NaNO_3$ in atmospheric $pCO_2$ after (A) ultrapure water rinse, (B) HCl pretreatment, (C) hydroxylamine HCl pretreatment and (D) peroxide pretreatment.*

*Cr(VI) sorption on montmorillonite*

Cr(VI) sorption kinetics on untreated montmorillonite (Swy-2 from the Clay Minerals Society) were measured for equilibration times of up to 1 week. At pH 3, Cr(VI) sorption was rapid, reaching 100% for a $10^{-5}$ M Cr(VI) solution on 30 g/L montmorillonite in 0.1, 0.01 or 0.001 M $NaNO_3$ within a few hours (Figure 8A). However, sorbed Cr(VI) did not desorb at pH 10, even after several days. Experiments testing reversibility demonstrated that negligible Cr(VI) sorbed at an initial pH of 10 (see also Figure 8C). Reversing an initial pH of 10 to pH 3 resulted in rapid Cr(VI) uptake; this Cr(VI) remained irreversibly sorbed for subsequent acid/base titration cycles (Figure 8B).

Pretreatment of montmorillonite with peroxide (as above for kaolinite) produced dramatic changes in Cr(VI) sorption rates and quantities. Very little Cr(VI) sorbed on peroxide-washed montmorillonite, with no significant change in sorption occurring as pH

was cycled between pH 3 and 10. These results suggest that trace organic matter, or more likely, Fe(II) in the montmorillonite lattice, is responsible for the irreversible sorption of Cr(VI). As for kaolinite, we hypothesize that Cr(VI) is reduced and strongly adsorbed as Cr(III). This hypothesis will need to be tested using further experiments, for example, relying on XAS or Mossbauer spectroscopy.

Cr(VI) sorption edges spanning a range of 3 to 10 were measured on untreated montmorillonite. In one set of experiments ("I" on Figure 8C), individual reactors were titrated to initial pH values spanning the range of pH before introducing the montmorillonite. In a second set of experiments, aliquots were drawn from a batch slurry ("B" on Figure 8C) as it was rapidly titrated from pH 3 to 10, with aliquots subsequently equilibrated for periods of up to 1 week, as in experiments with γ-alumina, HMO and kaolinite. The batch slurry and individual reactors produced similar results: at pH <7, Cr(VI) sorption increased steadily for at least one week. Close agreement between ICP and UV/Vis measurements of aqueous Cr demonstrated that all Cr in solution was present as Cr(VI).

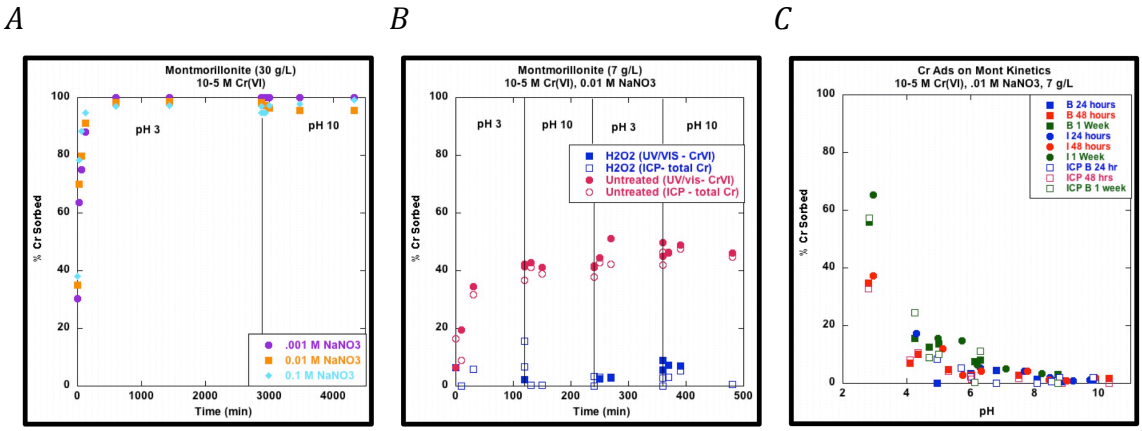


*Figure 8. Cr(VI) adsorption on montmorillonite in ambient atmosphere. (A) $10^{-5}$ M Cr(VI) adsorption on 30 g/L montmorillonite in 0.001, 0.01 or 0.1 M $NaNO_3$ at an initial pH of 3 and after titration to pH 10, (B) $10^{-5}$ M Cr(VI) adsorption on 7 g/L montmorillonite in 0.01 M $NaNO_3$ with no pretreatment (red) or pretreatment with 30% $H_2O_2$ solution (blue) for an initial pH 3 and subsequent titration to pH 10, 3 and 10, and (C) $10^{-5}$ M Cr(VI) adsorption on 7 g/L montmorillonite in 0.01 M $NaNO_3$ for reaction times of 24 hrs to 1 week.*

Rate experiments completed with both kaolinite and montmorillonite resulted in non-equilibrium, irreversible sorption. Furthermore, pretreatment of the clays with hydroxylamine HCl, HCl or peroxide dramatically changed the adsorption of Cr(VI), particularly at acidic pH. Therefore, the adsorption edges cannot be correctly modeled using thermodynamically-based surface complexation models, which assume equilibrium has been achieved. Further investigation, beyond the scope of this study, will be required to understand these processes more fully. Without such investigation, it may be difficult or impossible to model Cr(VI) adsorption on natural sediments and soils containing clay minerals using a component additivity approach.

*Cr(VI) sorption on mineral mixtures*

Adsorption edges of Cr(VI) were measured on goethite mixed with kaolinite, montmorillonite, hydrous ferric oxide, hydrous manganese oxide or γ-alumina as a function of pH from 3.5-10, in 0.01 M $NaNO_3$ with 0-5% $pCO_2$. Edges were also measured for mixtures of all solids using equal surface areas (60-150 $m^2/g$) as function of $pCO_2$ and ionic strength. Goethite and hydrous ferric oxide were synthesized according to methods in Schwertmann and Cornell (1991, Iron Oxides in the Laboratory) and characterized using 11 pt $N_2$ BET and powder X-ray diffractometry.

As for Cr(VI) adsorption on pure goethite, adsorption on the mixtures increased with decreasing pH at pH<9, reaching 100% adsorption at low pH (Figures 9, 10). Cr(VI) adsorption on the pure goethite and on the solid mixtures decreased with increasing $pCO_2$ (Figure 9). The kinetics of adsorption were examined by measuring Cr(VI) adsorption edges after 24 hr, 48 hr, 1 week or 2 weeks of reaction time. Adsorption was rapid for all solid mixtures, with little change in sorption from 24 hrs to 2 weeks (Figure 10).

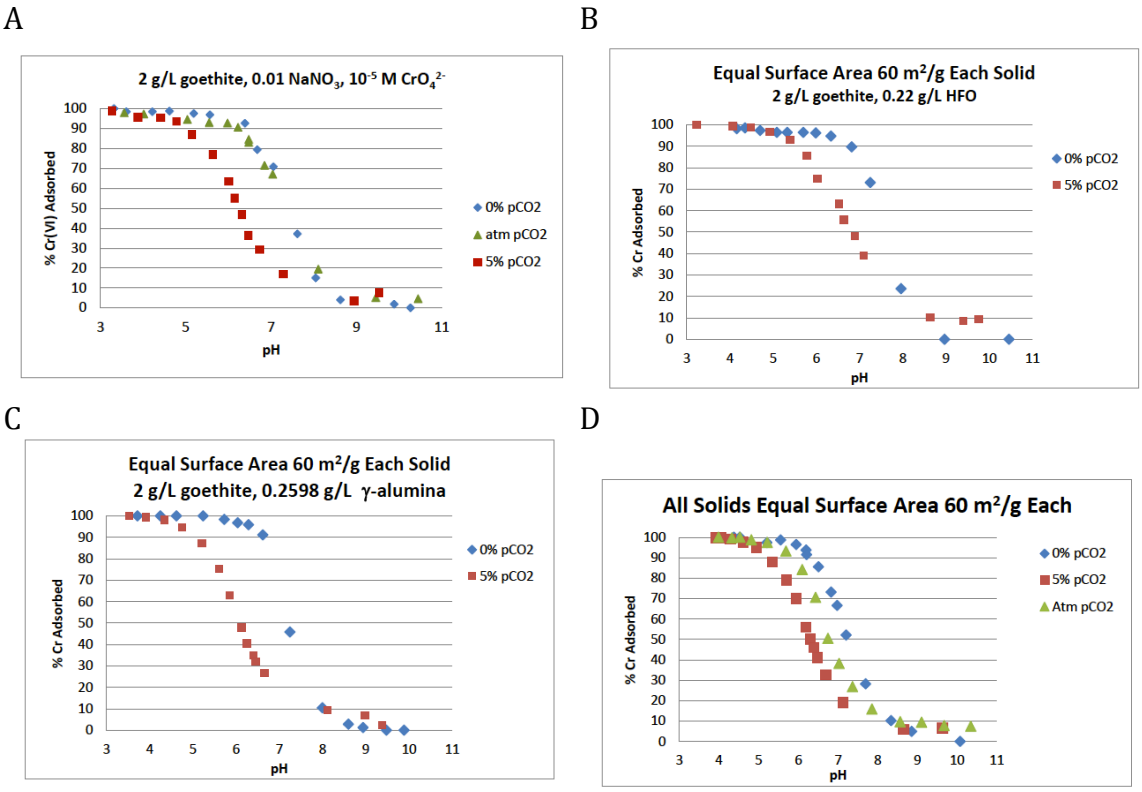


*Figure 9. Cr(VI) adsorption ($10^{-5}$ M) edges measured on (A) 2 g/L goethite or 2 g/L goethite with (B) 0.22 g/L HFO, (C) 0.2598 g/L γ-alumina and (D) 0.222 g/L HFO, 0.09 g/L HMO, 0.258 g/L γ-alumina, 4.12 g/L kaolinite and 1.875 g/L montmorillonite at 0% $pCO_2$ (blue), atmospheric $pCO_2$ (green) or ~5% $pCO_2$ (red) in 0.01 M $NaNO_3$.*

A

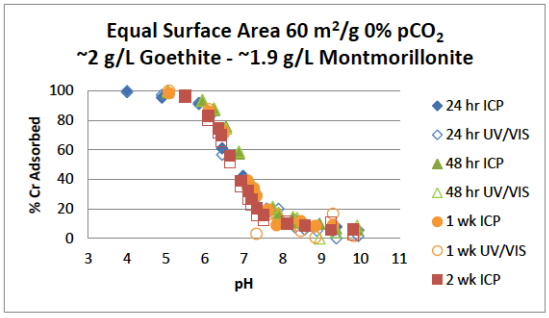


B

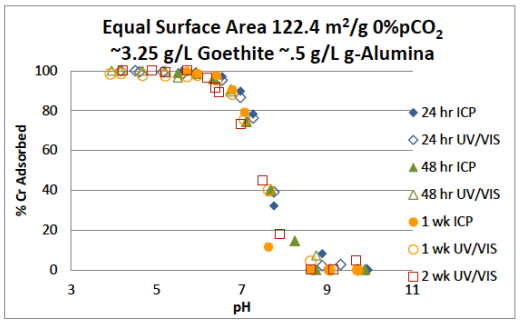


C

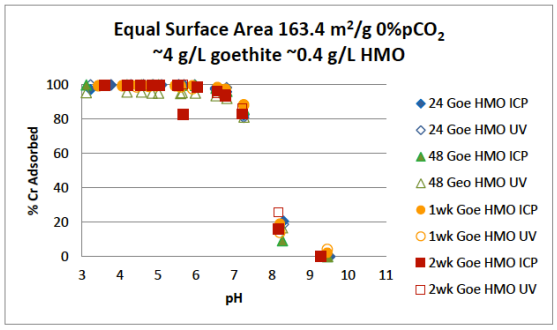


D

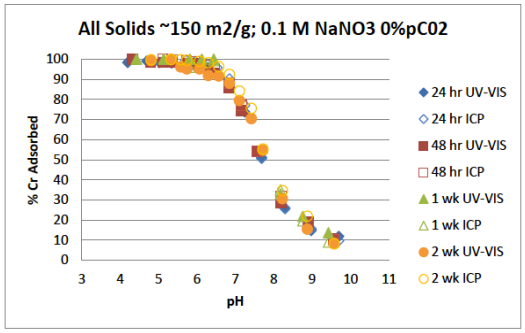


*Figure 10. Cr(VI) adsorption ($10^{-5}$ M Cr) edges measured on (A) 2 g/ goethite and 1.9 g/L montmorillonite, (B) 3.25 g/L goethite and 0.5 g/L γ-alumina, (C) 4 g/L goethite and 0.4 g/L HMO and (D) 2 g/L goethite and 0.2598 g/L γ-alumina and (D) 2g/L goethite, 0.222 g/L HFO, 0.09 g/L HMO, 0.258 g/L γ-alumina, 4.12 g/L kaolinite and 1.875 g/L montmorillonite under 0 $pCO_2$ from 24 hrs to 2 weeks reaction time.*

A simple component additivity approach was used to predict Cr(VI) adsorption in the mixed mineral systems. Diffuse layer surface complexation models were used to describe Cr(VI) adsorption on each solid. Model predictions for mixtures of goethite with γ-alumina, HFO and HMO were in very good agreement with measured edges (Figure 11). For kaolinite and montmorillonite, as described above, adsorption did not reach a clear equilibrium for the simple endmember systems. Nonetheless, Gilchrist (2013) used a single edge for each untreated clay to derive Cr(VI) adsorption stability constants (Figure 12). Perhaps unsurprisingly, component additivity model predictions based on these relatively unconstrained endmember DLMs produced poorer fits compared to the other mixed solid systems. For both kaolinite and montmormillonite mixtures with goethite, Cr(VI) adsorption was overestimated by the component additivity model (Figure 12).

A.

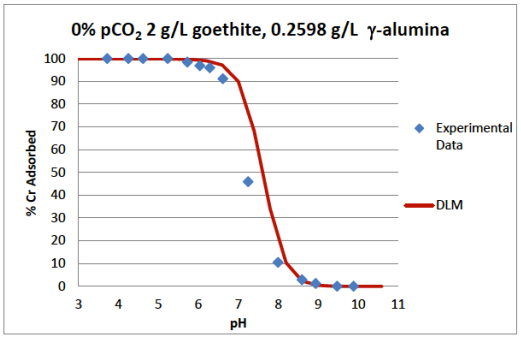


B.

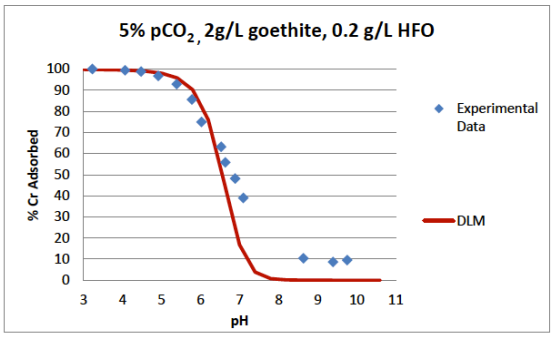


C.

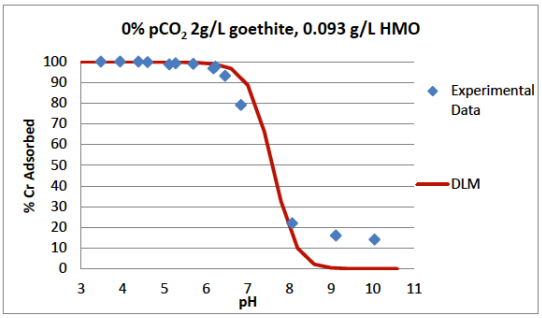


*Figure 11. Adsorption edges for $10^{-5}$ M Cr(VI) on 2 g/L goethite with (A) 0.2598 g/L γ-alumina, (B) 0.2 g/L HFO and (C) 0.093 g/L HMO in 0.01 M $NaNO_3$. Lines indicate DLM predictions using a component additivity approach with models developed for the pure solid systems (goethite model from Gilchrist, 2013; γ-alumina model from Reich and Koretsky, 2011; HFO model from Dzombak and Morel, 1990; HMO model from MacLeod, 2013).*

*A.* *B.*

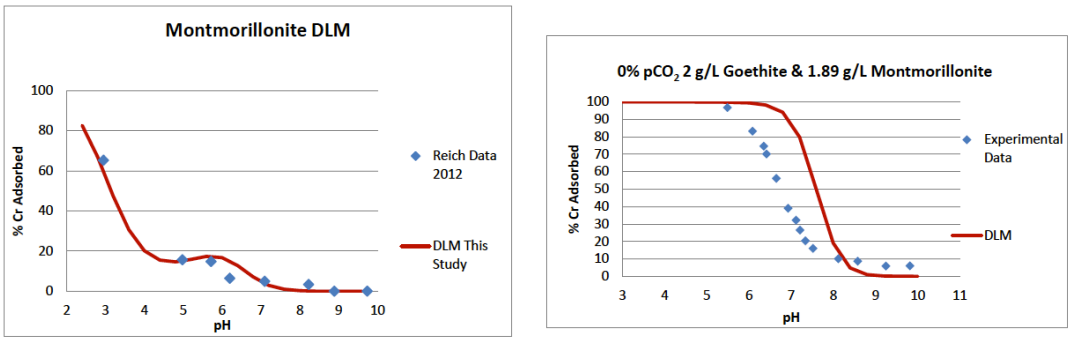


*C.* *D.*

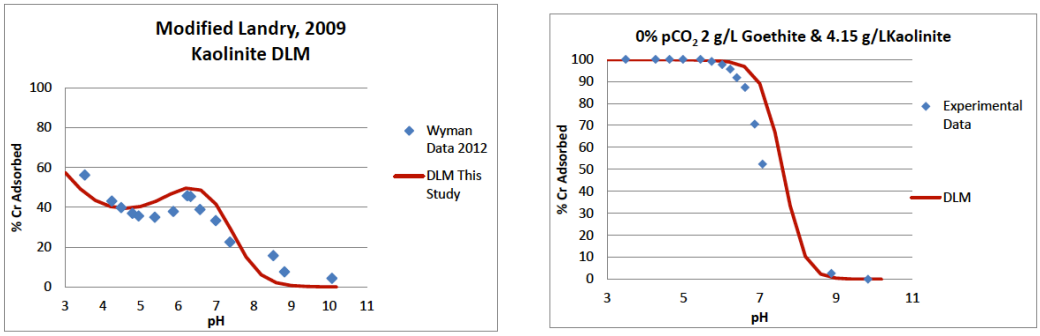


*Figure 12. Adsorption edges for $10^{-5}$ M Cr(VI) on (A) 7 g/L montmorillonite, (B) 2 g/L goethite and 1.89 g/L montmorillonite, (C) 30 g/L kaolinite and (D) 2 g/L goethite and 4.15 g/L kaolinite in 0.01 M $NaNO_3$. Lines in (B) and (D) indicate DLM predictions using a component additivity approach with models developed for the pure solid systems, as shown in (A) and (C).*

A component additivity approach was also used to predict Cr(VI) adsorption on mixtures containing equal surface areas (60 or 150 $m^2/g$ each) of all six solids. Each individual solid DLM was incorporated into the thermodymamic database of the speciation code MINTEQ. However, MINTEQ can only calculate speciation for a system containing a maximum of five solid surfaces. Calculations were completed to determine the solid expected to contribute least to adsorption in the mixed mineral system, and this solid (HMO) was not included in the calculations. Model predictions for the mixtures containing the larger quantities of solids (higher total surface area) and higher ionic strength were in excellent agreement with the measured adsorption edges (Figure 13 A-C). Cr(VI) adsorption at low $pCO_2$ is predicted to be controlled by HFO and goethite, with HFO adsorption an increasing fraction of the Cr(VI) with increasing pH (Figure 13A, B). At high $pCO_2$, HFO is predicted to adsorb a greater fraction of the Cr(VI) than at lower $pCO_2$ (Figure 3A-C). Overall predictions of Cr(VI) adsorption were also very good for the lower ionic strength and lower surface area mixtures at the highest $pCO_2$, but the total Cr(VI) adsorption was overestimated at lower $pCO_2$ (Figure 13D-E). HFO and goethite were still predicted to be the dominant sorbents for Cr(VI) in lower ionic strength/lower surface area experiments.

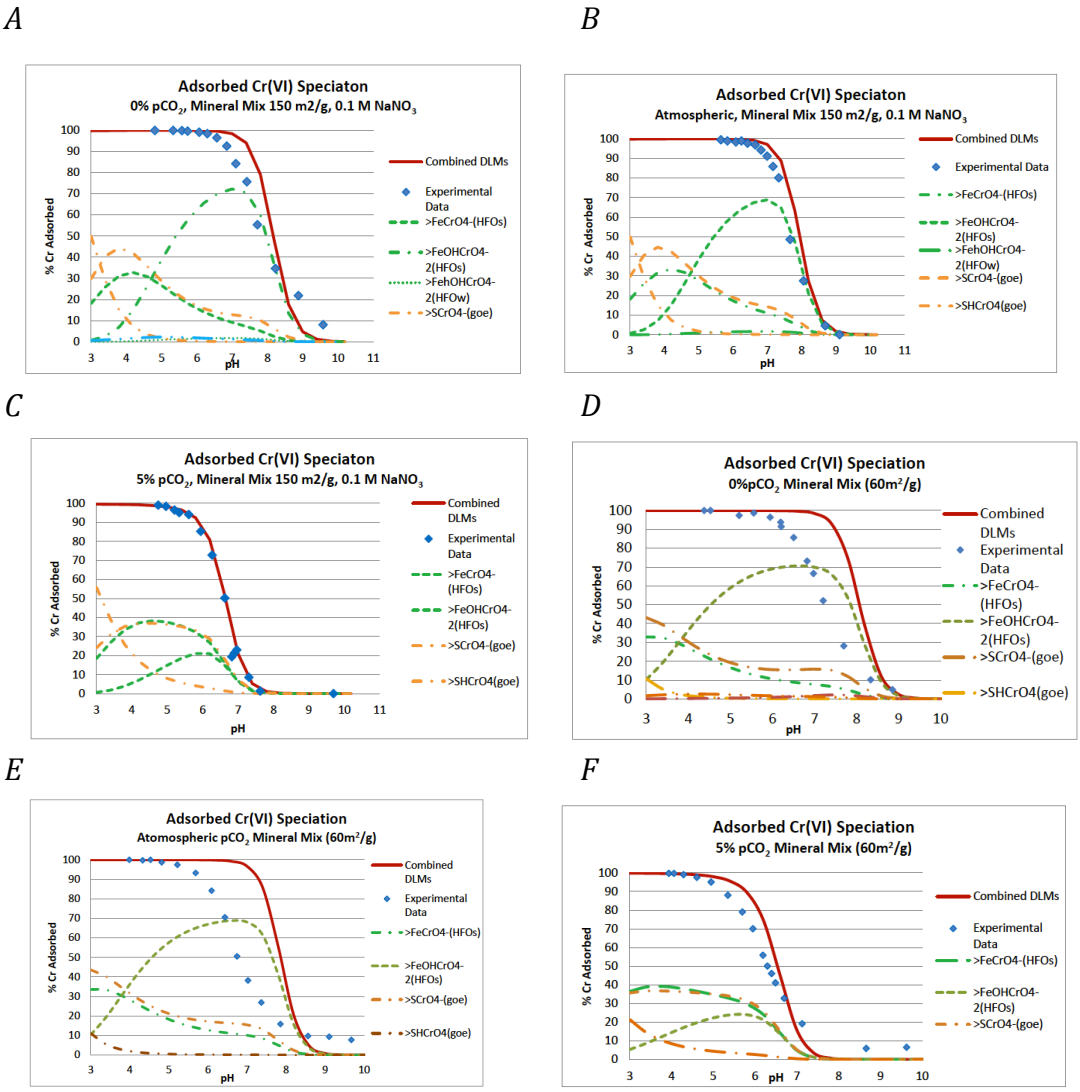


*Figure 13. Adsorption edges for $10^{-5}$ M Cr(VI) on mixtures of all six solids. Red lines indicate component additivity predictions for each system based on DLMs derived for the individual solids. Total surface area of solids in (A)-(C) experiments was 150 $m^2/g$ and in (D)-(F) was 60 $m^2/g$.*

*Cr(VI) sorption on natural sediments*

Sediment cores (50 cm length) were collected from a minerotrophic fen (Kleinstuck Marsh, Kalamazoo, MI). The upper 10 and lower 10 cm of ~10 cores were combined into two sample sets and used for subsequent study. The initial organic carbon content of the 40-50 cm interval was estimated to be 65% based on loss-on-ignition at 550°C (Figure 14). Sequential extractions were completed according to a procedure adapted from Tessier et al. (1979; 1982). This extraction sequentially targets and removes solids and associated trace metals associated with four operationally-defined fractions: exchangeables ($MgCl_2$

reagent), carbonates (sodium acetate reagent), reducibles (hydroxylamine HCl reagent) and oxidizables (hydrogen peroxide reagent). The extracted supernatant from each step was analyzed for a suite of ions via ICP-OES (Na, Ca, Mg, K, Mn, Fe), and the remaining sediments was analyzed using LOI and used in adsorption experiments (see below). The organic matter content remained relatively stable with removal of the operationally defined exchangeable, carbonate and reducible fractions, but decreased to ~20% after removable of the oxidizable fraction (Figure 14). The largest quantity of Fe was extracted with the reducible and oxidizable fractions, presumably representing Fe hydroxides and Fe associated with organic matter, respectively (Figure 15). Mn was extracted mostly with the exchangeable and carbonate fractions, with smaller quantities associated with the reducible fraction. K is mostly extracted with the exchangeables fraction, due to release from clay minerals, and Ca and Mg are mostly released with the carbonates fraction, as expected (not shown).

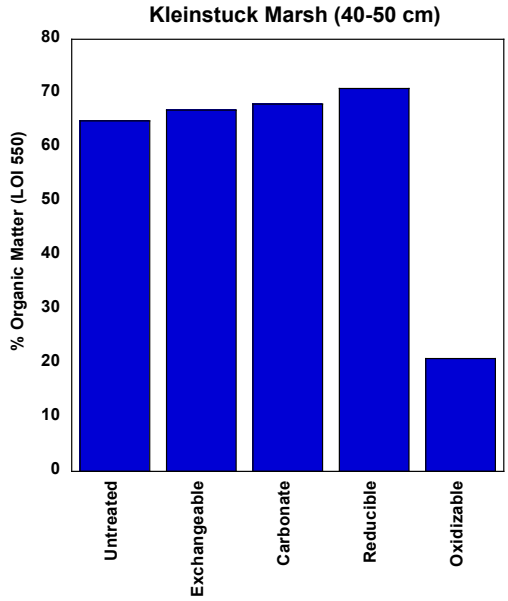


*Figure 14. Initional loss-on-ignition (550°C, 2 hrs) from 40-50 cm interval of Kleinstuck Marsh sediments, and after stepwise removal of four operationally-defined fractions (Wyman et al., 2012).*

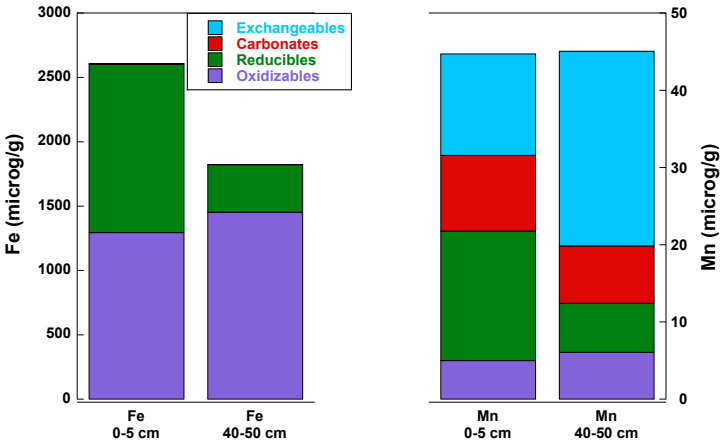


*Figure 15. Sequential extraction of Fe and Mn from organic-rich Kleinstuck Marsh sediments (Wyman et al., 2012).*

After each successive extraction step, a portion of the extracted sediment was reserved for use in adsorption edge measurements. Cr(VI) adsorption edges were measured on the bulk sediment and on sediments after successive extraction of the four targeted fractions (Figure 15). Adsorption experiments were conducted using $10^{-5}$ M Cr(VI), pH 3-10, with 0.01 M $NaNO_3$ and as a function of time (24 hrs, 48 hrs, 1 week and 2 weeks). For all sediments except those with the oxidizable portion extracted, Cr(VI) sorption increases with time below pH 7, reaching a maximum of 100% sorbed at pH 3 and decreasing with increasing pH. Below pH 7, comparison of total aqueous Cr ICP-OES and aqueous Cr(VI) UV/Vis spectrophotometric data demonstrates that all Cr remaining in solution is Cr(VI). In contrast, above pH 7, Cr(III) in solution increases with time, with the largest increases occurring at the highest pH. Cr(VI) adsorption edges on sediments with the oxidizable pool extracted are distinct from those on all other sediments; after 2 weeks, a maximum of 50% of the Cr(VI) sorbs at pH 3, with <20% sorbed between pH 4 and 7. This suggests that much of the Cr(VI) binds to organic matter or other reduced fractions of the soil (e.g. Fe(II)-bearing clays). Adsorption of Cr(III) on the bulk sediment demonstrates that Cr(III) adsorption is rapid, reaching nearly 100% at pH≤6 in 24-48 hrs, and decreasing with increased pH to ~30% sorbed at pH 9 (data not shown). These data are consistent with the hypothesis that Cr(VI) is reduced by organic matter or Fe(II) in the sediment at alkaline pH and is slowly released to solution. Because the largest change in Cr(VI) adsorption was observed with removal of the organic fraction, component additivity predictions of Cr(VI) adsorption based on the inorganic fractions was not attempted.

Adsorption edges for Cr(VI) on sandy, organic-poor ($LOI_{550}$ < 2%)sediments from the Rifle Integrated Field Research Challenge site were also measured. Cr(VI) adsorption increased greatly with decreasing pH, and showed little dependence on ionic strength (Figure 16). Adsorption may have increased slightly between 24 and 48 hr equlibration time, but differences in the edges were close to experimental error of ~5%. After removal of the exchangeable fraction, Cr(VI) adsorption decreased to <5% at all pH and remained low after subsequent removal of carbonate, reducible and oxidizable fractions. More work needs to be done on this system to determine if the loss in adsorption capacity was due to chemical changes in the sediment or loss of the finest fraction of the sediments during the extraction process. This needs to be resolved before a component additivity approach can be applied to Cr(VI) adsorption on these sediments.

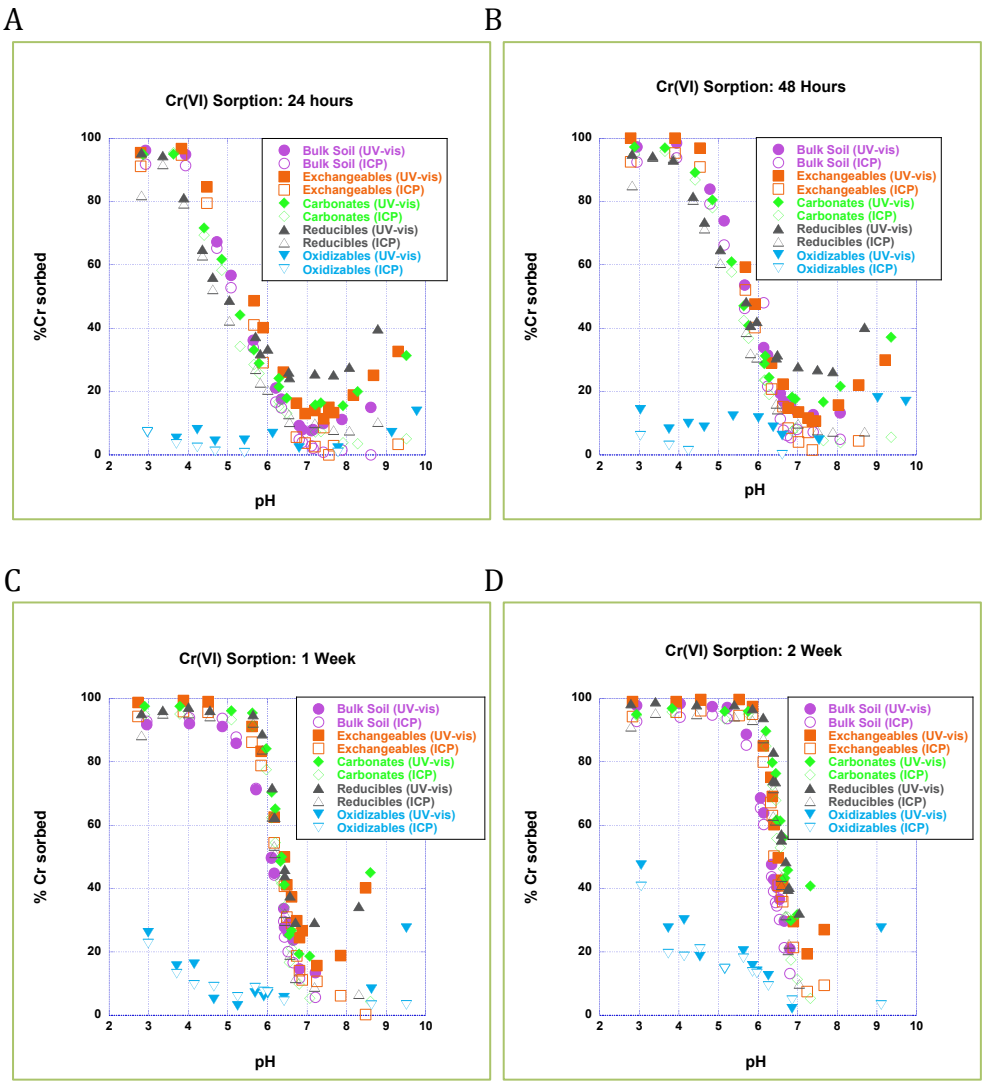


*Figure 15. Adsorption of Cr(VI) on organic-rich Kleinstuck Marsh sediments after successive extraction of four operationally-defined fractions with equilibration times of 24 hrs to 2 weeks(Wyman et al., 2012). Quantity sorbed calculated using total Cr in solution (open symbols; ICP data) or Cr(VI) in solution (closed symbols; UV/vis data).*

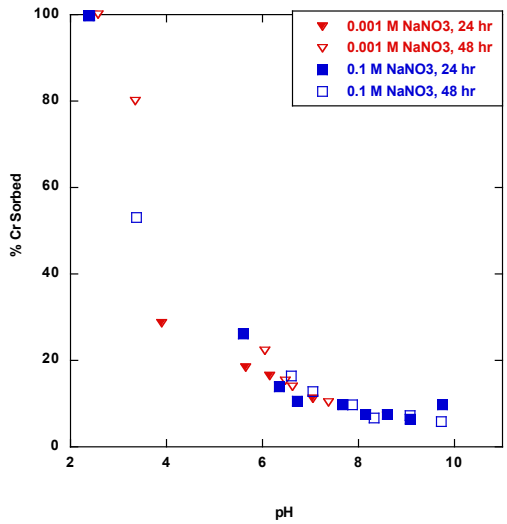


*Figure 16. Adsorption of $10^{-5}$ M Cr(VI) on 20 g/L Rifle site sediments in 0.001 M $NaNO_3$ (red) or 0.1 M $NaNO_3$ (blue) with equilibration times of 24 hrs (closed) to 48 hrs (open).*

## PRODUCTS PRODUCED:

*Journal Articles:*

Reich T. and Koretsky C.M. (2011) Cr(VI) adsorption on γ-alumina in the presence and absence of $CO_2$: comparison of surface complexation models. *Geochimica et Cosmochimica Acta*, 75, 7006-7017.

*Journal Articles In Preparation:*

MacLeod A. and Koretsky C.M. Adsorption of Cr(VI) on hydrous manganese oxide. For submission to Chemical Geology (anticipated submission date: January 2013)

Gilchrist A. and Koretsky C.M. Adsorption of Cr(VI) on mineral assemblages. For submission to Chemical Geology (anticipated submission date: February 2013)

*Masters Theses:*

MacLeod A. (2013) Adsorption of hexavalent chromium on hydrous manganese oxide Department of Geosciences, Western Michigan University, Kalamazoo, MI.

Gilchrist A. (2013) Surface Complexation Modeling of Cr(VI) Adsorption on Mineral Assemblages. Department of Geosciences, Western Michigan University, Kalamazoo, MI.

*Conference Presentations:*

Koretsky C.M., Gilchrist A.M., MacLeod A., Reich T.J. and Wyman D. (2013) Development of surface complexation models for natural and model mineral assemblages. 12th International Conference on the Biogeochemistry of Trace Elements. Athens, GA, June 16-20.

Gilchrist A.M. and Koretsky C.M. (2012) Sorption of Cr(VI) on mineral assemblages of goethite with clays and Al-oxides. Goldschmidt Conference, Montreal, Canada, June 24-29.

Koretsky C.M. (2012) Adsorption of metals and oxyanions on mineral assemblages. Goldschmidt Conference, Montreal, Canada, June 24-29.

Wyman D., Koretsky C.M. and Barger M.L. (2012) Cr(VI) adsorption on organic rich soil from Kleinstuck Marsh, Kalamazoo, MI. Goldschmidt Conference, Montreal, Canada, June 24-29.

Koretsky C.M. and Reich T.J. (2011) Cr(VI) adsorption on γ-alumina. Goldschmidt Conference, Prague, Czech Republic, August 14-19.

MacLeod A. and Koretsky C.M. (2011) Adsorption of Cr(VI) on hydrous manganese oxide. Goldschmidt Conference, Prague, Czech Republic, August 14-19.